LATVIAN JOURNAL OF PHYSICS AND TECHNICAL SCIENCES
2017, N 5

DOI: 10.1515/lpts-2017-0031

# DYNAMIC AIR GAP CHANGE OF LOW-SPEED GENERATOR CONSIDERING THERMAL EXPANSION, CENTRIFUGAL FORCE AND MAGNETIC FORCE EFFECTS

M. Cerpinska, R. Elmanis-Helmanis
Riga Technical University,
1 Kalku Str., Riga LV-1658, LATVIA
e-mail: marina.cerpinska@rtu.lv

The paper provides the data collected over a three-year period to illustrate the dynamic air gap change depending on generation modes of four hydropower generators with similar design. The tests were performed on hydropower units at the rated apparent power of 105 MVA and the air gap of 20 mm. The results obtained showed that the average air gap change in different modes could reach up to 2.1 mm. Around 90 % of air gap change results from thermal expansion and 10 % were determined by centrifugal and magnetic forces. In coasting mode when the power was switched off and the speed of the generator decreased, the air gap increased up to 0.7 mm. Attraction forces resulting from magnetic phenomena accounted for 0.1–0.6 mm decrease in the air gap.

***Keywords:*** *air gap, centrifugal force, hydropower unit, magnetic force.*

## 1. INTRODUCTION

Knowing the exact value of operational air gap is important for two reasons. Firstly, applying the correct values of the air gap ensures correct modelling and simulation results for the transient parameters of electrical machines [1]. Secondly, it provides valuable information for reliability check of the equipment.

When the condition monitoring of the hydropower generator is performed, the air gap is measured and evaluated. The evaluation requires comparing the actual air gap to its nominal value or the average value. According to the Institute of Electrical and Electronics Engineers (IEEE) manual p. 8.5.1 [2], air gap variation of ±10 % from average is acceptable. It means that for the average air gap value of 20 mm, the distance between the rotor pole and stator could be either 18 mm or 22 mm. The static air gap of hydropower generator measured during the commissioning stage can be close to those required values, but the dynamic air gap measured during operation tends to vary more in different operational modes.

During the early measurements series in 2015, the minimum air gap measured on unit No. 1 in mode "Full speed no load (FSNL) excited 13.8 kV" was 18.1 mm, while the maximum air gap in mode "Coasting with 31 % rotational speed of rated speed" was 20.2 mm (see Fig. 4 for more details). The difference between average values in those modes was 2.1 mm, but the difference between the minimum and maximum value reached 3.64 mm. While the variation of the rotor roundness and static air gap due to imperfection of fabrication and balancing was intuitive, the idea of the rigid rotor assembly contracting or expanding during operation seemed unrealistic and provided motivation for further investigation.

Researchers agree that the dynamic air gap or the operating air gap is different from the static air gap because the rotating assemblies are subject to centrifugal and magnetic forces [3]–[4]. The thorough description of stresses of rotating discs was addressed in the Journal of Applied Mathematical Modelling [5], but the change of the air gap could not be explained by rotor stresses only. Since the air gap is a distance measurement between the rotor pole and stator bar, it is affected both by rotor and stator movement. Stator does not rotate, but it is subject to thermal expansion effects, and as noted three decades earlier, it is more deformable than rotor and yields to a variety of forces [4]. According to Chapter 2.6 [6], the forces in the stator frame and foundation are massive, especially during instantaneous changes in generation modes. Therefore, the objective of the paper was to study simultaneously the temperature effects and the impact of centrifugal and magnetic forces on the air gap.

The site measurements showed that the air gap either decreased when the load was applied to the generator (see results in Section 4.3) or increased when the speed of the generator decreased (see results in Section 4.2), but the main variation was determined by thermal expansion. Indeed, the manufacturers today specify the nominal or designed air gap value both for "cold" and "hot" generator in the technical documentation and the difference between the two could be from 1.5 to 2 mm (for the units under study the rated "hot" air gap was 20 mm, and "cold" air gap was 18 mm).

The experimental results of the paper discuss the underlying factors for dynamic air gap change and provide some data collected over a three-year period to illustrate the specific air gap values depending on generation modes of four low-speed salient pole synchronous generators of the same design. In addition, a comparison of the air gap change and vibration results is provided.

## 2. THEORY

### *Centrifugal Force*

The example of centrifugal force acting on a generator rotor is shown in Fig. 1. The model given in the handbook [7], which is adapted for particular design of units (size of assembly parts and bearing location), is discussed in the study.

The centrifugal force is not a concern of the small perfectly balanced rotating articles, but large generators (the units under study had rotor diameter of 11.62 m) on site could not realistically have zero unbalance, and therefore there is centrifugal force, while the unit rotates. The guidelines [8] provide an example for the ultimate situation when "at a runaway speed after a load rejection stresses can be three to four times higher than in rated operation".

The centrifugal force is proportional to the speed of the unit as suggested by dynamic equation (1) [9]:

$$F_c = mr\omega^2, \tag{1}$$

where $F_c$ – centrifugal force, *N*; *m* – eccentrically located mass centre of the rotor, *kg*; *r* – radius from eccentrically located mass to the rotation axis, *m*; $\omega$ – angular speed of rotation, *rad/s*.

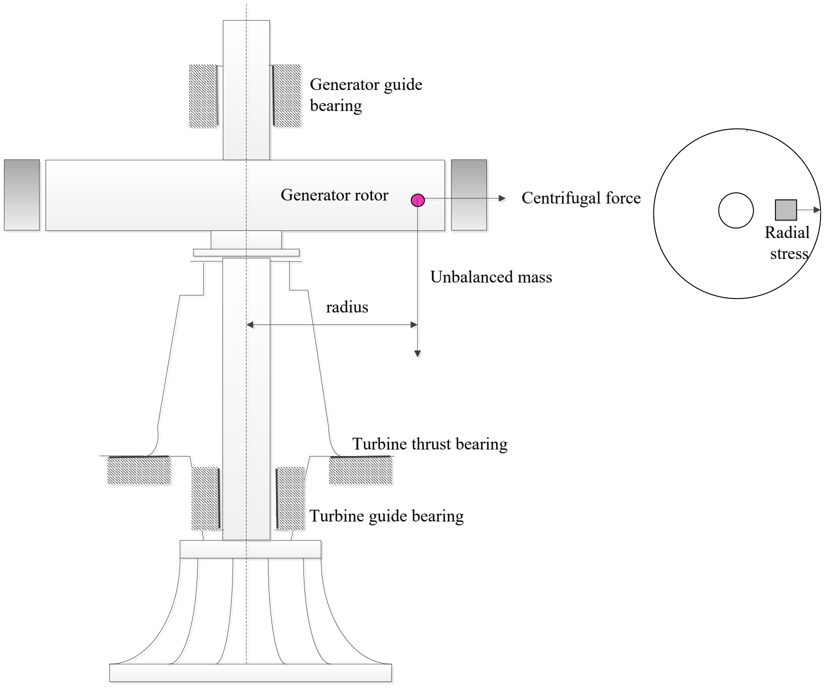


*Fig.1.* Design of the unit and bearing location. Centrifugal force vector acting on hydropower generator, causing rotor to expand radially.

Following equation (1), as the speed decreases, the centrifugal force decreases. The stresses developed due to rotation and centrifugal forces in circular disks are circumferential stresses $\sigma_c$ and radial stresses $\sigma_r$ [10]–[11]. Considering the direction of these stresses, the size of the air gap is affected by the radial stress. Radial stress for a rotating solid disk at any radius *r* is calculated according to equation (2) [11]:

$$\sigma_r = \frac{\rho \cdot \omega^2}{8}(3 + \mu)[r_2^2 - r^2], \tag{2}$$

where $\sigma_r$ – radial stress, *N/m²*; $\rho$ – density of material, *kg/m³*; $\omega$ – angular speed of rotation, *rad/s*; $\mu$ – Poisson's ratio; *r* – radius at any point of the disc, *m*.

Equation (2) shows that at a lower speed the radial stress developed due to the centrifugal force decreases because other variables do not change, since the radius is calculated from boundary conditions when stresses are zero [10]. Thus, the radial stress $\sigma_r$ developed in the rotating disc depends only on angular speed $\omega$ squared.

To describe centrifugal force effects, coasting mode (natural deceleration of a generator when the power is removed) was studied. In coasting mode, excitation is switched off and magnetic forces can be considered negligible, and mainly the centrifugal force is acting on the generator rotor. Modes at different rotational speeds were analysed, starting from the rated rotational speed until the crawling speed equal to ~30 % of rated operational speed was achieved.

*Magnetic Force*

If there is a change in vibration when the load is applied, it means that there are unbalanced electrical exciting forces acting on the generator. Equation (3) for magnetic force is given as [7]:

$$F_m = \frac{S}{2\mu_0} B^2, \tag{3}$$

where $F_m$ – magnetic force, *N*; *S* – section area of the rotor pole, $m^2$ ; $\mu_0$ – $4\pi \cdot 10^{-7}$, magnetic constant, also known as Vacuum Permeability, *H/m*; *B* – magnetic field, *T*.

Magnetic force was evaluated by comparing "FSNL excited/ non-excited" modes. In "FSNL non-excited" mode there are no magnetic forces acting on the generator, while in "FSNL excited" mode there is no current flow in stator windings, but magnetic current is produced by the excitation windings [12].

*Hydraulic Forces*

Synchronous condenser or "condense" mode is compared with "FSNL non-excited" mode to study the effect of hydraulic forces because in synchronous condenser mode there is no water flow affecting the turbine [7]. For the present study, synchronous condenser mode with 0 MVAr reactive power supplied back to the electrical grid was used.

## 3. EXPERIMENTAL PART

The tests were performed on four 105 MVA, 13.8 kV, 50 Hz hydropower units with umbrella-type hydrogenerators. Generator rotors had 68 salient rotor poles, rotor spider with 12 segments, rotation direction – clockwise. Stator had 14.62 m diameter and six segments with 504 stator slots. The rated speed of the units was 88.2 RPM. Nominal air gap was 20 mm. The design of the unit and bearing location is shown in Fig. 1. The design of the generator rotor is demonstrated in Fig. 2.

The "Meggitt Vibro-Meter air-gap" measurement system ILS730 with sensor LS120 (sensitivity 0.3V/mm (±5 %), range 0–33 mm) was used. The value of the air gap is measured in Volts and converted to millimetres according to manufacturer's scale. In the earliest experiments of 2014–2016, two air gap sensors were used, placed at the top and at the bottom of the stator; in 2017 four sensors were used, placed at the top of the rotor as shown in Fig. 2. Thus, two air gap sensors were used for generators No. 1 and No. 2. Four sensors were used for generators No. 3 and No. 4. Using more sensors allows for better analysis of the dynamic behaviour in case of unbalance. Table 1 summarises the history and location of the sensors for the present study.

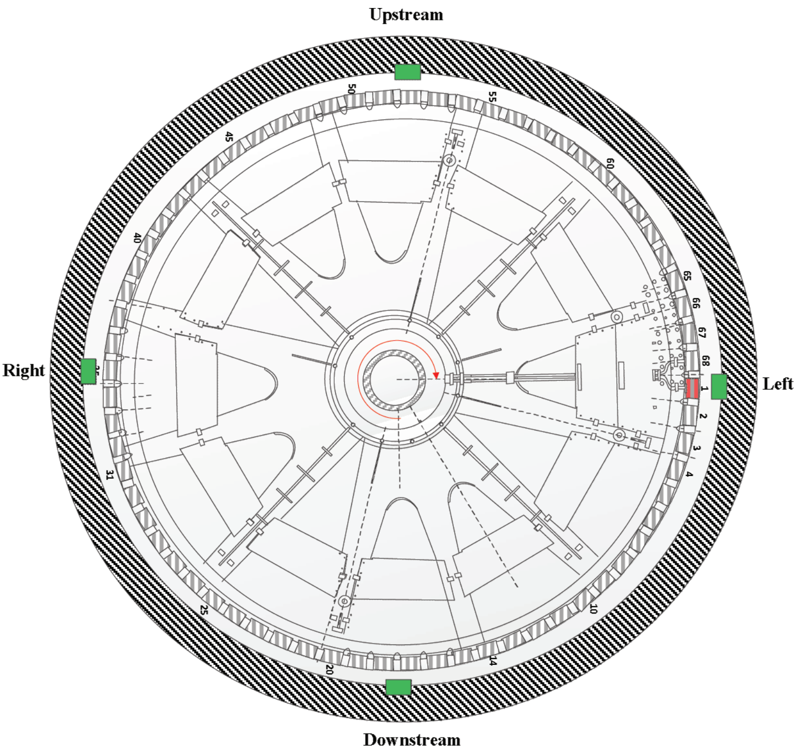


*Fig.2.* The top view of generator rotor and four air gap sensors (indicated green) are glued at the top of the stator. The first rotor pole is indicated red.

*Table 1*

**Sensor Positions for Experiments**

| No. | Year | Unit | Measurement position |
|---|---|---|---|
| 1 | 2014 | No. 1 | 1 sensor on top |
| 2 | 2015 | No. 1 | 2 sensors (top and bottom, see Fig. 1 in [13]) |
| 3 | 2015 | No. 1 | 2 sensors on top |
| 4 | 2016 | No. 2 | 2 sensors (top and bottom) |
| 5 | 2016 | No. 2 | |
| 6 | 2017 | No. 3 | 4 sensors on top |
| 7 | 2017 | No. 4 | |

The units are presented in consecutive order in the paper according to measurement dates to meet the confidentiality policy of the owned power plant. The results in the following section are provided in the same sequence.

Invasive sensors glued on the stator provide good precision, but the stator roundness should be considered when absolute values of the air gap in millimetres are conferred because stators in practice are rarely thoroughly even. Stator roundness was checked by attaching an invasive air gap sensor to one of the rotor poles, placing the measurement equipment inside the rotor for data recording and rotating the generator at a crawling speed. As a result, variation of measurement results from four sensors could be logically explained. The example of unit No. 3 is provided in Fig. 3, where downstream sensor air gap values were always greater than upstream values.

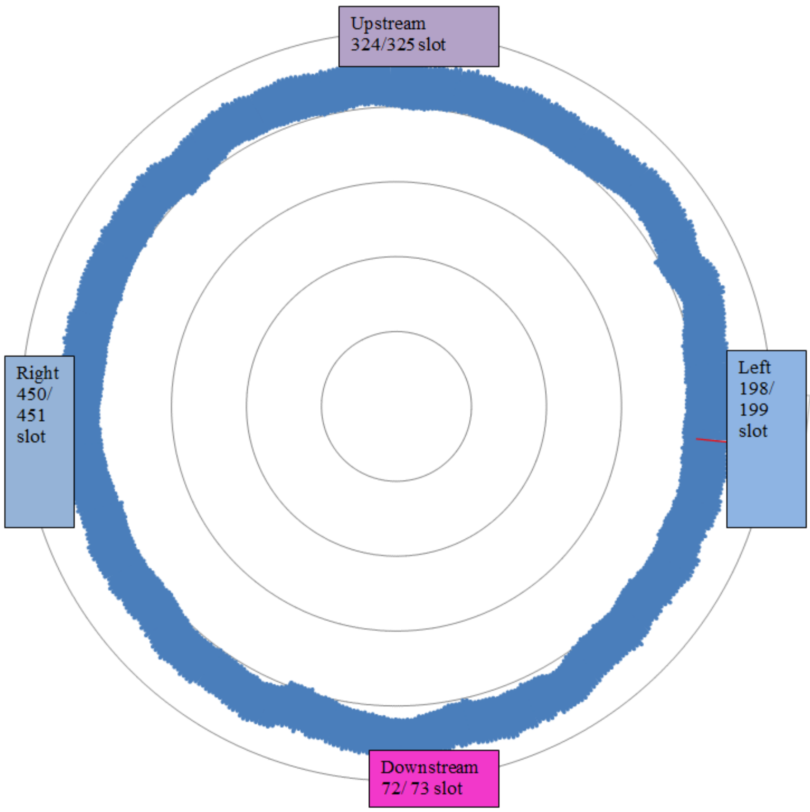


*Fig.3.* Stator shape, example for Unit No. 3, explaining different results of the air gap obtained from different sensors. The downstream sensor readings give the greatest value. Left and right sensor readings are the same.

## 4. RESULTS

The example of change of the average air gap in different generation modes is shown in Fig. 4, where the change depending on temperature is also demonstrated. Stator core temperature was obtained from the built-in condition monitoring system.

### *4.1. Temperature Change Effects on the Air Gap*

Observations on site and expertise of other researchers investigating air gap size [14] suggested that the air gap changed significantly as the stator temperature changed; therefore, the variation of the air gap during the generator warm-up and different modes was registered. The results are shown below in Fig. 4 for unit No. 1.

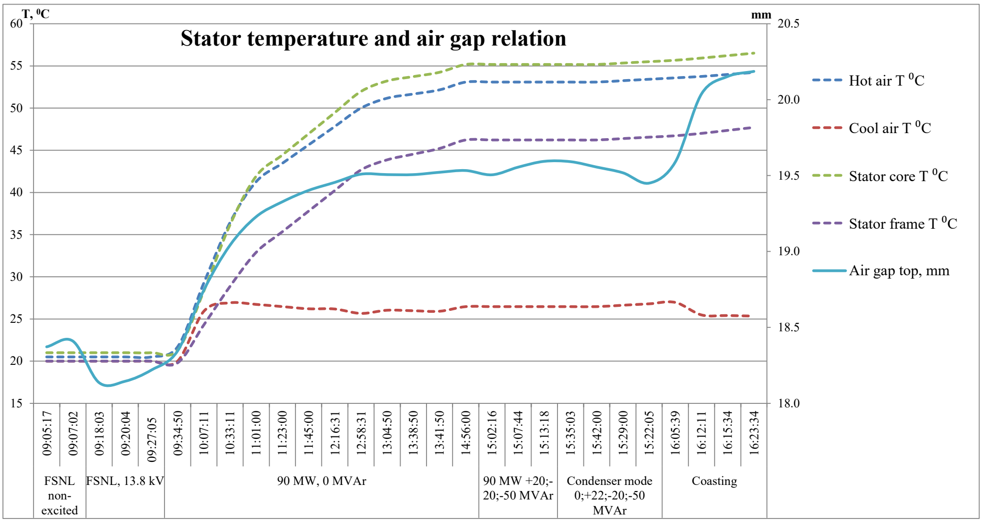


*Fig.4.* Air gap change in different operating modes.

The air gap change from temperature is best observed in mode “90 MW, 0 MVAr”, when no other changes were applied to the unit. Correlation of air gap change and temperature change and stator wall movement due to thermal expansion was calculated, based on the sample correlation coefficient and the coefficient of determination [15]. Results are summarised in Table 2.

*Table 2*

**Correlation of Air Gap Change from Temperature Change and Stator Wall Thermal Expansion for Unit No. 1**

| Correlation of air gap with: | Hot air T, °C | Cool air T, °C | Stator core T, °C | Stator frame T, °C | Displacement of the stator wall (relative to stator core) |
|---|---|---|---|---|---|
| Sample correlation coefficient, *r* | 1.0 | 0.8 | 1.0 | 0.9 | 0.9 |
| Positively correlated, $r > 0$? | yes | | | | |
| Coefficient of determination | 91 % | 69 % | 91 % | 90 % | 83 % |
| Correlation strength | strong | week | strong | strong | strong |

Although correlation measures association rather than causation, Table 1 together with Fig. 4 provides good evidence that 83 % of air gap growth can be explained by stator expansive displacement during warm-up, 7 % of air gap growth is caused by other thermal expansion phenomena or other underlying factors, and the remaining 10 % is determined by forces independent of temperature, such as centrifugal and magnetic forces.

*4.2. Centrifugal Force Effect on the Air Gap*

Figure 3 suggests that especially in coasting mode the change of the air gap could not be explained by the temperature change because temperature remains the same, while the air gap value grows. As suggested in the theory section, the centrifugal forces are the main factors acting on the generator during the coasting mode. It means that in this specific mode the correlation between angular velocity and the air gap should be strong. The results of the air gap of units No. 1, No. 2 and No. 3 in coasting mode provided in Table 3 justify this statement.

*Table 3*

**Correlation of Air Gap at Speed in Coasting Mode of Units No. 1, No. 2 and No. 3**

<table>
<tr><td rowspan="9">Unit No. 1</td><td>Speed, % of rated operation</td><td>Speed, RPM</td><td>Average air gap, top sensor</td><td>Average air gap, bottom sensor</td></tr>
<tr><td>100 %</td><td>88.2</td><td>19.00</td><td>20.09</td></tr>
<tr><td>64 %</td><td>56.6</td><td>19.44</td><td>20.56</td></tr>
<tr><td>48 %</td><td>42.7</td><td>19.56</td><td>20.68</td></tr>
<tr><td>40 %</td><td>35.6</td><td>19.59</td><td>20.72</td></tr>
<tr><td colspan="2">Sample correlation coefficient, r</td><td>-0.99</td><td>-0.99</td></tr>
<tr><td colspan="2">Positively correlated, r > 0?</td><td colspan="2">No, negatively correlated</td></tr>
<tr><td colspan="2">Coefficient of determination</td><td>98 %</td><td>98 %</td></tr>
<tr><td colspan="2">Correlation strength</td><td>strong</td><td>strong</td></tr>
<tr><td rowspan="10">Unit No. 2</td><td>Speed, % of rated operation</td><td>Speed, RPM</td><td>Average air gap, top sensor</td><td>Average air gap, bottom sensor</td></tr>
<tr><td>100 %</td><td>88.0</td><td>23.12</td><td>24.50</td></tr>
<tr><td>87 %</td><td>77.0</td><td>23.47</td><td>24.85</td></tr>
<tr><td>63 %</td><td>56.0</td><td>23.69</td><td>25.10</td></tr>
<tr><td>52 %</td><td>45.5</td><td>23.76</td><td>25.17</td></tr>
<tr><td>49 %</td><td>43.0</td><td>23.77</td><td>25.18</td></tr>
<tr><td colspan="2">Sample correlation coefficient, r</td><td>-0.96</td><td>-0.96</td></tr>
<tr><td colspan="2">Positively correlated, r > 0?</td><td colspan="2">No, negatively correlated</td></tr>
<tr><td colspan="2">Coefficient of determination</td><td>92 %</td><td>93 %</td></tr>
<tr><td colspan="2">Correlation strength</td><td>strong</td><td>strong</td></tr>
<tr><td rowspan="10">Unit No. 3</td><td>Speed, % of rated operation</td><td>Speed, RPM</td><td colspan="2">Average air gap of top upstream sensor, mm</td></tr>
<tr><td>60 %</td><td>52.9</td><td colspan="2">21.67</td></tr>
<tr><td>50 %</td><td>44.1</td><td colspan="2">21.76</td></tr>
<tr><td>44 %</td><td>38.8</td><td colspan="2">21.79</td></tr>
<tr><td>39 %</td><td>34.4</td><td colspan="2">21.81</td></tr>
<tr><td>35 %</td><td>30.9</td><td colspan="2">21.82</td></tr>
<tr><td colspan="2">Sample correlation coefficient, r</td><td colspan="2">-0.97</td></tr>
<tr><td colspan="2">Positively correlated, r > 0?</td><td colspan="2">No, negatively correlated</td></tr>
<tr><td colspan="2">Coefficient of determination</td><td colspan="2">94 %</td></tr>
<tr><td colspan="2">Correlation strength</td><td colspan="2">strong</td></tr>
</table>

The negative correlation in Table 3 indicates that for this data set a speed which is less than the rated speed is strongly associated higher than the designed value of the air gap. This is explained by equation (1) since the centrifugal force is smaller, when the rotation speed is lower.

Some values obtained for unit No. 2 appeared to be unreasonably large. Since the measured value of the air gap depends on earthing quality of the capacitive air gap sensor, the real values of air gap of unit No. 2 could be less. Nevertheless, the tendency of air gap change due to a decrease in the rotational speed is still conclusive.

### *4.3. Magnetic Pull Effect on the Air Gap*

The difference between modes "FSNL non-excited" and "FSNL excited 13.8 kV" is distinct in Fig. 3. As soon as the load is applied to the generator, the air gap decreases. This is due to the fact that a magnetic phenomenon present in "FSNL excited 13.8 kV" mode produces forces of attraction, which act on the rotor and the stator. The specific decrease is shown in Table 4 (please see measurement positions and measurement years in Table 1).

*Table 4*

**Results of Change in Air Gap in Modes Switching from "FSNL non-excited" to "FSNL excited 13.8 kV"**

| No. | Difference, average in mm | Comments on vibration |
|---|---|---|
| 1 | -0.3 | Vibration was approximately the same. |
| 2 | -0.3 | |
| 3 | -0.3 and -0.6 | |
| 4 | -0.5 | |
| 5 | -1.1 and -1 | Vibration significantly increased on turbine thrust bearing. Temperature effects disrupted this experiment because when the mode of FSNL 13.8 kV was measured, the generator was still "cold". |
| 6 | -0.1, -0.2, -0.3 | Vibration increased both on generator guide bearing and turbine thrust bearing. |
| 7 | -0.1 and -0.2 | Vibration was greater on turbine thrust bearing in "non-excited" mode. |

### *4.4. Hydraulic Forces*

To evaluate hydraulic effects, "Synchronous condenser" and "FSNL excited 13.8 kV" modes were chosen so that magnetic pull was similar in both modes, and additional unbalance was caused by hydraulic forces in "FSNL excited 13.8 kV" mode only. Results are shown in Table 5.

*Table 5*

**Results of Change in Air Gap and Vibration in Modes “Synchronous Condenser” and “FSNL Excited 13.8 kV”**

| No. | Air gap | Vibration |
|---|---|---|
| 1 | No distinctive difference | Greater in FSNL excited mode |
| 2 | Smaller in FSNL excited mode by 0.3 mm | Greater in FSNL excited mode |
| 3 | Greater in FSNL excited mode by 0.2 mm | No distinctive difference |
| 4 | Smaller in FSNL by 0.5 mm | Greater in FSNL excited mode |
| 5 | Generator was “cold” in one mode, data could not be used for comparison | Significantly greater in FSNL excited mode |
| 6 | No distinctive difference | Greater in FSNL excited mode |
| 7 | No distinctive difference | Significantly greater in FSNL excited mode |

Vibration data in Table 5 illustrate that in condenser mode there is no water on the turbine, so the vibration values are smaller. Results 6 and 7 are the most informative because for those generators vibration was much higher in FSNL excited mode than in synchronous condenser mode, while air gap remained the same.

## 5. DISCUSSION

If the air gap were the same in all operation modes, it would have meant that the stator and rotor expanded uniformly. In the example of unit No. 1 in Fig. 3, the stator expanded faster than the rotor.

Some displacement data, omitted in the results section, showed that during the coasting mode the stator contracted a little bit due to the drop of cooling air flow temperature. On the contrary, the hot air did not change and the air gap increased as the generator speed decreased – Table 2 showed the strong negative correlation of speed and air gap size. The low speed was strongly associated with higher than designed value of the air gap. Equation (1) showed that the higher the speed, the higher the centrifugal force. Applying this principle to the coasting mode, at a speed of 43 RPM, the centrifugal force would be 24 % of the centrifugal force for the generator at the rated rotational speed of 88.2 RPM, and at the crawling speed of 34 RPM, the centrifugal force would be only 15 % compared to the rated speed. However, when less tensile outward forces act on the rotor poles, the rotor of hydropower generator could contract up to 0.7 mm during the crawling speed compared to its size in the rated operation.

Although the attraction forces resulting from magnetic phenomena are considered to be large [4], [16], the difference of the air gap after the load applied to the generator was not more than 0.6 mm. This is a little bit less than 1 mm (the value suggested by early developers of air gap measurement systems [4]).

## 6. CONCLUSIONS

1. The air gap growth during operation proved to be determined by stator expansive displacement during warm-up in the first place. The thermal expansion effects caused 90 % of the air gap variation.
2. In coasting mode the air gap growth proved to be determined by the decrease in speed of the generator and decrease of centrifugal force and resulting radial stress. The increase of the air gap up to 0.7 mm was registered at the crawling speed compared to the rated speed of rotation.
3. Magnetic phenomena accounted for 0.1–0.6 mm air gap change for the generators with nominal air gap of 20 mm. When magnetic forces were applied, the air gap became smaller due to attraction forces.
4. Hydraulic forces had no effect on the air gap during the present study. The change of turbine bearing vibration remained the best indicator of hydraulic force effects.

## REFERENCES


1. Kokoko, O., Merkhouf, A., Tounzi, A., Al-Haddad, K., & Guillot, E. (2015). Analysis of air-gap influence on a large hydro generator's parameters using sudden symmetrical short-circuit test. In 2015 IEEE International Electric Machines & Drives Conference (IEMDC), 10–13 May 2015 (pp. 102–107). Coeur d'Alene, USA: IEEE. DOI: 10.1109/IEMDC.2015.7409044
2. IEEE Std 492™-1999 (R2011). IEEE Guide for Operation and Maintenance of Hydro-Generators.
3. Adamowski, J. C., Souza, A. T., Perez, N., Lima, A. A., Oda, P. D., & Tiba, H. H. (2013). Ultrasonic dynamic air-gap monitoring system for large hydro-generators. In IEEE Joint UFFC, EFTF and PFM Symposium, 21–25 July 2013 (pp. 1311–1314). Prague, Czech Republic: IEEE. DOI: 10.1109/ULTSYM.2013.0335
4. Talas, P., & Toom, P. (1983). Dynamic measurement and analysis of air gap variations in large hydroelectric generators. *IEEE Transactions on Power Apparatus and Systems*, *v. PAS-102*(9), 3098–3106. DOI: 10.1109/MPER.1983.5519300
5. Allam, M. N. M., Badr, R. E., & Tantawy, R. (2008). Stresses of a rotating circular disk of variable thickness carrying a current and bearing a coaxial viscoelastic coating. *Applied Mathematical Modelling, 32*(9), 1643–1656. DOI: 10.1016/j.apm.2007.06.002
6. Klempner, G., & Kerszenbaum, I. (2004). *Operation and Maintenance of Large Turbo-Generators* (Vol. 14). Hoboken, New Jersey: John Wiley & Sons.
7. Shtern, E. P. (1985). *Handbook on operation and repair of hydraulic turbine equipment*. Moscow: Energoatomizdat (In Russian: Справочник по эксплуатации и ремонту гидротурбинного оборудования / под ред. Е. П. Штерна. М.: Энергоатомиздат).
8. VDI 3839 Part 6. (2007). *Instructions on Measuring and Interpreting the Vibration of Machines – Typical Vibration Patterns with Machine Sets in Hydraulic Power Stations*.
9. Vinogradov, O. (2000). *Fundamentals of kinematics and dynamics of machines and mechanisms*. Boca Raton, Florida: CRC press.
10. Jindal, U. C. (2010). *Machine design*. India: Pearson Education.

11. Bansal, R. K. (2009). *A textbook of strength of materials* (4th ed.). New Delhi: Laxmi Publications.
12. Dirba, J., Ketners, K., Levins, N., & Pugacevs, V. (2002). Electric Vehicles in Transport: Textbook. Riga: Jumava. (In Latvian: Dirba, J., Ketners, K., Levins, N., Pugačevs, V. (2002). *Transporta elektriskās mašīnas: mācību līdzeklis*. Rīga: Jumava).
13. Griscenko, M., & Elmanis-Helmanis, R. (2015). Eccentricity of slow-speed salient-pole generator: Analysis based on air gap spectrum. *Latvian Journal of Physics and Technical Sciences, 52*(1), 26–37. DOI: 10.1515/lpts-2015-0003
14. Aguiar, A. B. M., Merkhouf, A., & Al-Haddad, K. (2012). Influence of the air gap length on the magnetic core loss in large hydro generator. In 20th International Conference on Electrical Machines (ICEM), 2–5 September 2012 (pp. 328–332). Marseille, France: IEEE. DOI: 10.1109/ICElMach.2012.6349886
15. Ross, S. M. (2004). *Introduction to probability and statistics for engineers and scientists* (3rd ed.). USA: Elsevier Academic Press.
16. Dirani, H. C., Merkhouf, A., Giroux, A. M., & Al-Haddad, K. (2014). Study of the impact of eccentricity in large synchronous generator with finite elements. In International Conference on Electrical Machines (ICEM), 2–5 September 2014 (pp. 277–282). Berlin, Germany: IEEE. DOI: 10.1109/ICELMACH.2014.6960193

## HIDROAGREGĀTA ĢENERATORA DINAMISKĀS GAISA SPRAUGAS IZMAIŅAS TERMISKĀS IZPLEŠANĀS, CENTRBĒDZES UN MAGNĒTISKO SPĒKU IETEKMĒ

M. Čerpinska, R. Elmanis-Helmanis

### Kopsavilkums

Darbā ir apkopoti rezultāti, kas iegūti četriem vienādas uzbūves hidroagregātu ģeneratoriem triju gadu laikā, pētot dinamiskās gaisa spraugas izmaiņas, atkarībā no darba režīmiem. Pārbaudes veiktas hidroagregātiem ar nominālo pilno 105 MVA jaudu un 20 mm gaisa spraugu. Iegūtie rezultāti liecina, ka gaisa sprauga dažādos darba režīmos var vidēji izmainīties par 2.1 mm. Aptuveni 90% no gaisa spraugas izmaiņas ir skaidrojamas ar termiskās izplešanās procesu, bet 10% ir skaidrojamas ar centrbēdzes un magnētisko spēku ietekmi. Izskrējiena režīmā, kad slodze tiek noņemta, un rotācijas ātrums pakāpeniski samazinās, gaisa spraugas palielinājums var būt līdz 0.7 mm. Magnētisko pievilkšanās spēku ietekmē gaisa spraugas samazinājums var būt no 0.1 līdz 0.6 mm.

04.07.2017.